The International Journal of Advanced Manufacturing Technology
https://doi.org/10.1007/s00170-026-18250-y

ORIGINAL ARTICLE

Differential hot stamping of USIBOR® 1500 steel: effect of partial tool heating on phase transformation, hardness and springback

Camila Pereira Lisboa[1,2] · Richard Thomas Lermen[2] · Rafael Luciano Dalcin[3] · Marco Antonio Colosio[4] · Luana de Lucca de Costa[1] · André Rosiak[1] · Juliano Boeira Ercolani[1] · Renan da Silva Ramalho[1] · Lirio Schaeffer[1]

Received: 4 April 2026 / Accepted: 28 April 2026

Abstract
This study investigates the thermo-mechanical response of USIBOR® 1500 steel subjected to differential hot stamping using partial tool heating. Real-time temperature measurements, cooling rate analysis, microhardness mapping, and optical microscopy were employed to establish process–structure–property relationships under non-isothermal conditions. Increasing tool temperature (100–300 °C) reduces local cooling rates in the heated regions, promoting a transition from predominantly martensitic to mixed martensitic–bainitic and bainitic-dominated microstructures. This transition is accompanied by a decrease in hardness from approximately 470 $HV_{0.2}$ to 326 $HV_{0.2}$. Partial tool heating also affects springback behavior, inducing a mensurable shift toward negative springback due to asymmetric thermal contraction and phase transformation-induced strains. The results demonstrate that partial tool heating provides an effective and controllable strategy for tailoring local mechanical properties and springback response in press-hardened steel components.

Keywords Hot stamping · Tailored hot stamping · Differential cooling · USIBOR® 1500 · Tool temperature · Springback

1 Introduction

The increasing demand for improved vehicle safety, reduced fuel consumption, and lower greenhouse gas emissions has driven the extensive adoption of advanced high-strength steels (AHSS) in automotive body-in-white structures [1, 2]. These materials enable significant weight reduction while maintaining or enhancing crashworthiness [3]. However, their limited formability at room-temperature and the pronounced springback observed during cold forming impose constraints on dimensional accuracy, geometry complexity, and process robustness [4, 5].

In cold forming conditions, springback is strongly influenced by the high elastic modulus, elevated yield stress,

✉ Rafael Luciano Dalcin
rldalcin@gmail.com

Camila Pereira Lisboa
lisboa.cp@gmail.com

Richard Thomas Lermen
richard.lermen@gmail.com

Marco Antonio Colosio
marco.colosio@gm.com

Luana de Lucca de Costa
luanadldcosta@gmail.com

André Rosiak
andre.rosiak@ufrgs.br

Juliano Boeira Ercolani
julianoercolani@gmail.com

Renan da Silva Ramalho
ramalho.renan16@gmail.com

Lirio Schaeffer
schaefer@ufrgs.br

[1] Metal Forming Laboratory (LdTM), Federal University of Rio Grande do Sul (UFRGS), Porto Alegre, RS, Brazil

[2] ATITUS Educação, School of Engineering and Applied Sciences, Postgraduate Program of Architecture and Urbanism, Passo Fundo, RS, Brazil

[3] Department of Mechanical Engineering, Horizontina College (FAHOR), Horizontina, RS, Brazil

[4] General Motors Mercosul, Materials Engineering, São Caetano do Sul, SP, Brazil

Published online: 06 May 2026

and anisotropic behavior of AHSS [6]. Accurate prediction of this phenomenon remains challenging and requires advanced constitutive descriptions, including anisotropic yield criteria and distortional hardening models [7]. Recent studies have demonstrated that such approaches significantly improve predictive capability, particularly in bending-dominated processes [6–8]. Nevertheless, even with advanced modeling, springback remains a critical limitation in the manufacturing of complex geometries [8].

In this context, hot stamping has emerged as a key manufacturing technology for producing ultra-high-strength steel components [2, 9]. By combining forming at elevated temperatures with in-die quenching, this process enables the fabrication of complex geometries with high dimensional accuracy, near-net shape capability, and significantly reduced springback [10, 11]. Under these conditions, the reduction in elastic modulus and flow stress at elevated temperatures contributes to minimizing elastic recovery [12]. However, these advantages are accompanied by increased process complexity, higher energy consumption, and potential surface degradation [10].

Conventional hot stamping of boron steels, such as USIBOR® 1500 (22MnB5-based), is typically designed to produce fully martensitic microstructures, resulting in homogeneous mechanical properties and tensile strengths exceeding 1500 MPa [11, 13]. Despite these advantages, modern automotive structures increasingly require components with spatially tailored mechanical properties [2, 14], where regions of high strength coexist with zones of enhanced ductility or energy absorption [15].

To address this demand, several tailored hot stamping strategies have been proposed, including tailored blanks, tailored heating, and tailored tooling concepts [15–17]. Among these approaches, the use of tools combining heated and cooled regions has attracted considerable attention, as it enables local control of cooling rates and phase transformation behavior without additional joining operations or post-processing steps [18–20]. This approach allows the development of components with graded microstructures and properties within a single forming operation [21].

Previous studies have demonstrated the feasibility of achieving locally tailored properties through differential cooling during hot stamping [17, 22]. Experimental and numerical investigations have confirmed that partial tool heating or cooling can effectively modify transformation pathways, leading to spatial variations in microstructure, hardness, and strength [22, 23]. Nevertheless, several scientific and technological aspects of differential hot stamping remain insufficiently understood [24, 25].

In particular, the phase transformation behavior under non-isothermal conditions is still not fully described [9, 16]. Most available models rely on simplified or isothermal approaches that do not capture the continuous thermal histories experienced in industrial hot stamping operations [26, 27]. Consequently, the prediction of microstructural evolution and hardness under differential cooling conditions remains limited.

Further, the quantitative relationship between spatially varying cooling rates, local microstructural evolution, and the resulting hardness gradients has not been systematically established [28, 29]. Although general trends have been reported [14, 30, 31], a physically consistent framework linking thermal boundary conditions to final properties is still lacking.

Another important aspect concerns the transition zones between heated and cooled tool regions, which are often neglected or only implicitly considered [15, 31, 32]. These regions exhibit gradual variations in cooling rate, leading to mixed microstructures and graded mechanical properties that may significantly influence stress redistribution and overall component performance [20, 33]. Their explicit characterization remains limited in the literature.

In addition, while tailored hot stamping is typically discussed in terms of strength and hardness gradients, its implications for springback under non-uniform thermal conditions are still not yet fully understood. Although hot stamping generally reduces springback [34, 35], this assumption is primarily valid under homogeneous thermal conditions. In differential hot stamping, the presence of thermal gradients, spatially varying phase transformations, and asymmetric residual stress distributions may lead to non-intuitive behaviors, including the occurrence of negative springback [36].

Moreover, springback should not be interpreted as a purely global or uniform response of the component. Recent studies have shown that local angular measurements may not fully capture the overall geometric deviation, highlighting the importance of considering spatial variability in deformation analysis [6–8]. This aspect becomes particularly relevant in processes involving strong thermal and microstructural gradients [37].

In this context, the present study provides a systematic experimental investigation of the hot stamping of USIBOR® 1500 steel under partial tool heating conditions. By imposing controlled thermal gradients between heated and cooled tool regions, the study establishes direct correlation between local thermal histories, non-isothermal phase transformation behavior, microstructural evolution, microhardness distribution, and springback response.

Particular emphasis is placed on the identification of transition zones based on thermal and hardness gradients, as well as on the analysis of springback under asymmetric thermo-mechanical conditions. The results contribute to the understanding of process–structure–property relationships

in differential hot stamping and demonstrate that partial tool heating is an effective strategy for tailoring both mechanical properties and springback behavior in press-hardened steel components.

2 Materials and methods

2.1 Material

The material investigated in this study was USIBOR® 1500 steel, supplied as 1.5 mm thick sheets. This press-hardenable steel is based on a 22MnB5 substrate and is delivered with an Al–Si coating, which acts as a barrier against oxidation and decarburization during austenitization and hot stamping.

The chemical composition (wt%) was determined by optical emission spectroscopy using a *Bruker Q2ION* spectrometer. The analysis was performed on the coated material without prior removal of the Al–Si layer, thus representing the effective composition of the industrial sheet. The measured chemical composition is presented in Table 1.

The initial microstructure was characterized by optical microscopy. Samples were ground using SiC papers (100–1200 grit), polished with 0.3 µm diamond suspension, and etched with 2% Nital. Observations were performed using an *Olympus GX51* optical microscope. The substrate exhibited of a typical ferritic–pearlitic microstructure [9], while the Al–Si coating thickness was approximately 30 µm. Representative micrographs are shown in Fig. 1(a, b).

Table 2 Measured mechanical properties of USIBOR® 1500 steel prior to heat treatment

Yield strength (MPa)	Tensile strength (MPa)	Elongation (%)
463 ± 30	621 ± 20	21 ± 1

The reported values correspond to the average of three tests

Tensile tests were conducted according to ASTM E8M [38] using an EMIC universal testing machine. Rectangular specimens (200 × 20 × 1.5 mm) with a gauge length of 50 mm were tested under displacement control at 10 mm/min. The measured mechanical properties are summarized in Table 2.

2.2 Hot stamping setup and processing conditions

Hot stamping experiments were carried out using a specially designed tooling system enabling differential cooling through partial heating, allowing controlled thermal gradients during forming and die quenching. The tooling consisted of a punch, die, and blank holder, with one region actively heated and the opposite region water-cooled. This configuration enabled spatial control of heat extraction and, consequently, of phase transformation behavior.

Forming tests were performed in a double-acting hydraulic press with a capacity of 200 kN capacity, operating at the maximum speed of 19.5 mm/s to minimize heat losses prior to tool contact. The tooling assembly and schematic representations are shown in Fig. 2(a–c).

Prior to forming, the blanks were austenitized in an electrically heated furnace at 1000 °C for 5 min to ensure

Table 1 Chemical composition of USIBOR® 1500 steel (% mass)

C	Mn	Cr	Nb	Ti	B	Fe
0.202	1.179	0.175	0.003	0.032	0.002	Balance

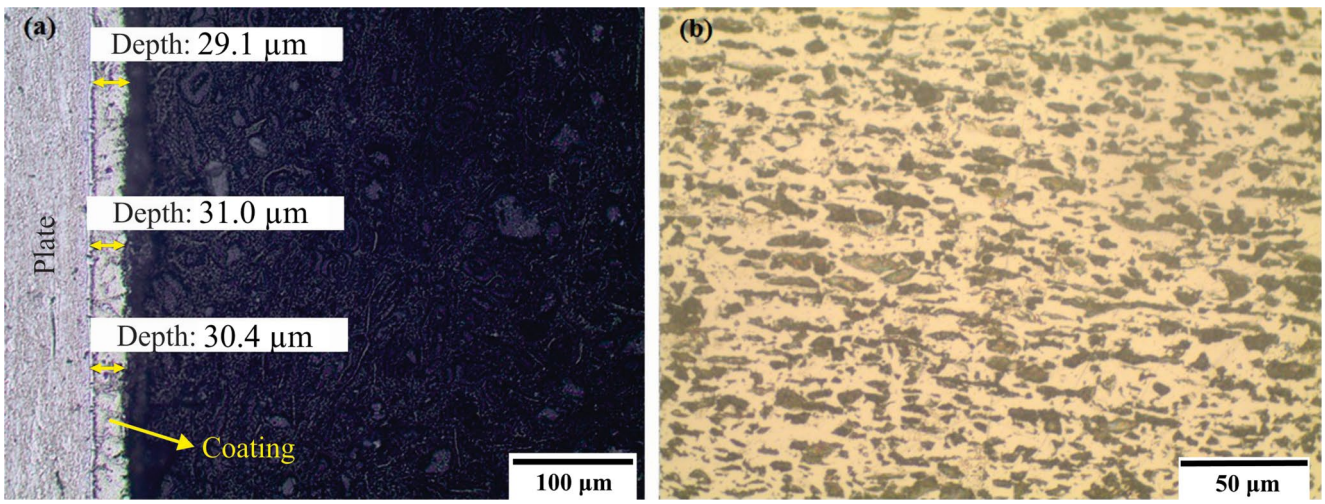

Fig. 1 Characteristics of USIBOR® 1500 steel prior to hot stamping and quenching: (**a**) Al–Si coating layer; and (**b**) base metal microstructure

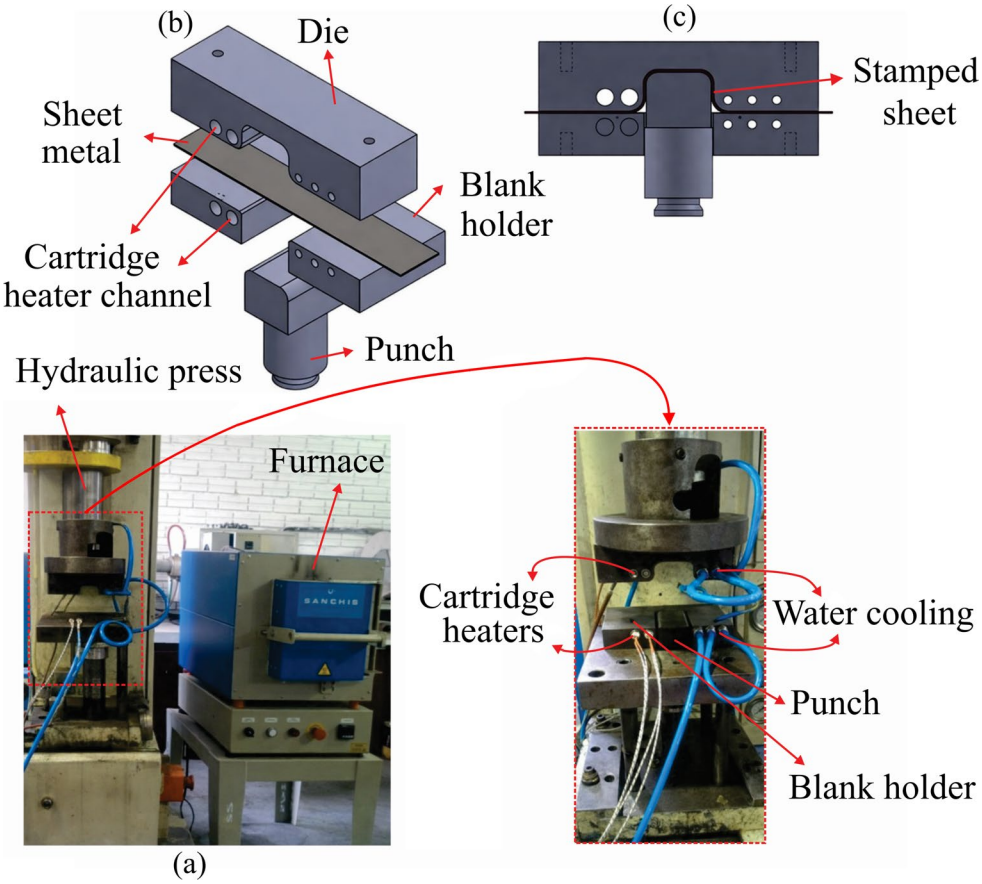

Fig. 2 Experimental tooling used in the stamping tests: (**a**) photograph of the heated die–punch assembly equipped with cartridge heaters and water-cooling system; (**b**) schematic exploded view of the tooling components, including die, punch, blank holder, cartridge heater channels, and cooling channels; (**c**) cross-sectional view illustrating the stamped sheet geometry and positioning used in the experiments

full austenitization. The temperature upon removal was approximately 930 °C. During transfer (4–6 s), the temperature decreased due to radiative and convective losses.

The actual forming temperature (600–650 °C) was experimentally measured using K-type thermocouples spot-welded to the blank surface. This value represents the real temperature at tool contact and was used for all thermal analyses. Although lower than typical industrial forming temperatures (700–800 °C), the measured cooling rates were sufficient to suppress diffusional transformations, as confirmed by thermal histories and the final microstructures.

After forming, the blank was held under full contact pressure for 10 s, during which forming and die quenching occurred simultaneously. This dwell time was selected based on industrial practice (8–15 s for 22MnB5 steels) [9, 10] and preliminary thermal measurements indicating complete cooling within this interval.

To ensure consistent interfacial heat transfer conditions, no lubricant was applied, and all tests were conducted under dry contact conditions. The tooling was manufactured from AISI H13 tool steel, quenched and tempered to a hardness of approximately 48–50 HRC.

Partial heating was achieved using four electrical cartridge heaters (500 W each, total 2 kW). Temperature was controlled using a PID system (±5 °C stability) and monitored by K-type thermocouples positioned near the tool–sheet interface. The experimental matrix is summarized in Table 3, where T_p denotes the furnace setpoint temperature, T_c the cooled tool region temperature, and T_h the heated tool region temperature.

Table 3 Experimental matrix for the different testing conditions

Condition	T_p (°C)	T_c (°C)	T_h (°C)
1	25	25	25
2	1000	25	25
3	1000	25	100
4	1000	25	200
5	1000	25	300

T_p – plate temperature, T_c – cold side temperature and T_h – hot side temperature of die and plate press

The cooled region was maintained at ~25 °C using a water-cooling system (5 L/min), and thermal insulation minimized lateral heat transfer. Five forming conditions were evaluated:

(i) Condition 1: cold stamping (25 °C);
(ii) Condition 2: conventional hot stamping (unheated tools);
(iii) Condition 3–5: partial tool heating at 100 °C, 200 °C, and 300 °C.

2.3 Temperature measurement and cooling curves

Thermal histories were obtained using K-type thermocouples for both tool and blank. Tool thermocouples were embedded in 0.8 mm diameter holes (~20 mm depth) positioned near the tool–sheet interface. Blank temperatures were measured using spot-welded thermocouples, enabling real-time monitoring during transfer, positioning, and quenching. The component geometry and thermocouple locations are shown in Fig. 3.

Data acquisition was performed using a *Lynx ADS2500* system with a sampling rate to capture rapid thermal transients during tool contact. Cooling rates were determined from the slope of temperature–time curves within relevant transformation intervals.

The experimental cooling curves were superimposed onto a transformation diagram of USIBOR® 1500 steel adapted from the literature. It should be emphasized that this diagram is used only as a qualitative reference, while the experimentally measured cooling curves represent the actual non-isothermal thermal paths governing phase transformation.

2.4 Microhardness and microstructural characterization

After stamping, specimens were sectioned transversely and prepared using standard metallographic procedures, followed by etching with 2% Nital.

Vickers microhardness ($HV_{0.2}$) measurements were performed using an *Insize ISH-TDV1000* hardness tester. Indentations were spaced every 5 mm along the stamped component, covering heated, transition, and cooled regions, as illustrated in Fig. 4. Three specimens per condition were analyzed, and average values with standard deviation were reported.

Microstructural characterization was carried out by optical microscopy at representative regions associated with distinct thermal histories (points 8, 20 and 32 in Fig. 4).

Due to the inherent limitations of optical microscopy for distinguishing bainite and martensite under continuous cooling conditions, the microstructural interpretation was based on a combined analysis of optical features, hardness values, and local cooling paths. Therefore, microstructural descriptions such as “predominantly bainitic” or “mixed

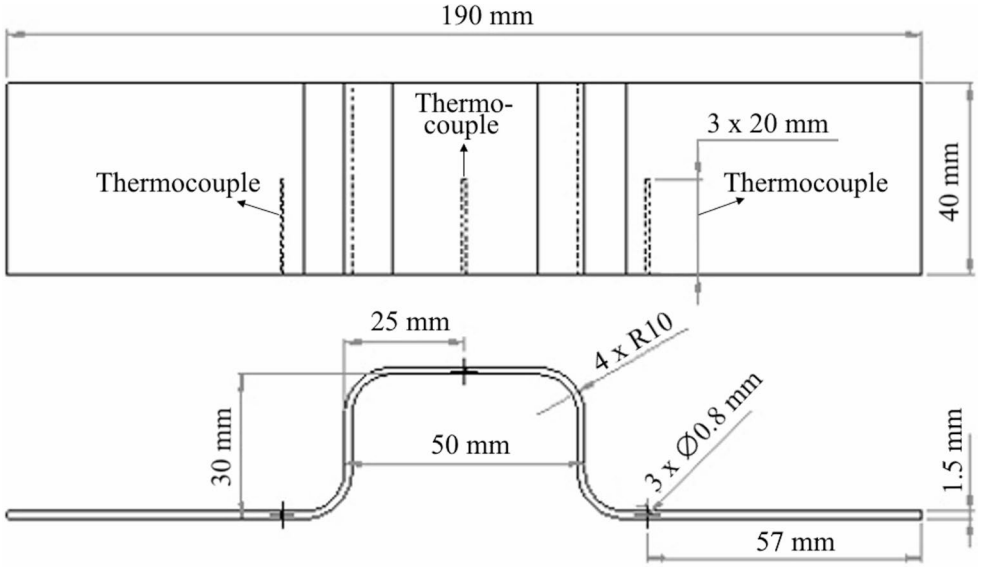

Fig. 3 Designed dimensions of the stamped component, indicating the locations and depths at which the thermocouples were inserted

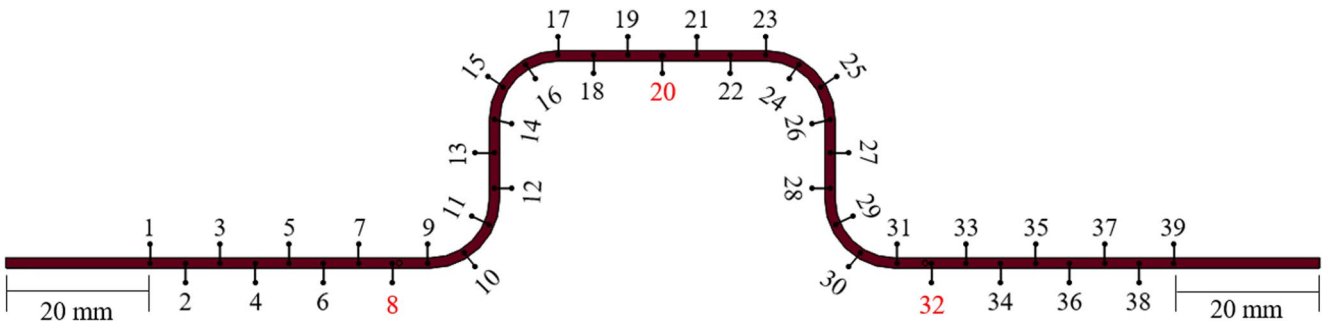

Fig. 4 Microhardness measurement points along with the stamped component

martensitic–bainitic" are used in a qualitative sense, as explicitly stated to avoid overinterpretation.

2.5 Springback measurement and statistical analysis

Springback was quantified using four angular measurements (θ_1–θ_4), from which springback values (α_1–α_4) were calculated as deviations from the nominal angle (90°), as illustrated in Fig. 5. These angles represent the final geometry of the component after unloading.

Digital images of the stamped components were acquired under controlled positioning conditions to minimize geometric distortions and analyzed using *SolidWorks*® software with consistent reference definitions. The selected measurement points correspond to regions subjected to distinct thermo-mechanical conditions, enabling spatial evaluation of springback behavior. In particular, angles located near the heated and cooled regions enable the assessment of asymmetric thermal effects induced by partial tool heating. For each processing condition, three specimens were analyzed, and the results are reported as mean values with corresponding standard deviations.

Although angular measurements provide a robust and widely adopted metric for comparative analysis in U-bending, they may not fully capture global geometric deviations. Therefore, the present approach is suitable for trend evaluation [34, 39], while full-field methods (e.g., 3D scanning) could provide a more comprehensive assessment.

Statistical analysis was performed using analysis of variance (ANOVA) to evaluate the effect of the stamping condition on the springback response. Prior to ANOVA, the assumptions of normality and homogeneity of variances were verified. Statistical significance was assessed at a 95% confidence level ($\alpha = 0.05$).

3 Results

3.1 Cooling behavior

Temperature measurements during forming enabled the construction of representative cooling curves for each hot stamping condition. These curves were superimposed onto a transformation diagram of USIBOR® 1500 steel to support the interpretation of phase transformation behavior under non-isothermal conditions.

Although commonly referred to as a time–temperature–transformation (TTT) diagram [40], the adopted representation incorporates features of continuous cooling transformation (CCT) behavior [40, 41]. Therefore, it is used here strictly as a qualitative reference, while the experimentally measured cooling curves represent the actual thermal paths governing phase evolution.

For conventional hot stamping (Condition 2), Fig. 6(a), forming was initiated at approximately 600–650 °C. Despite this relatively low temperature, the cooling rates upon tool contact were sufficiently high to suppress diffusional transformations. The cooling paths rapidly enter the martensitic transformation domain with minimal spatial variation along the component. This uniform thermal history results in a predominantly martensitic microstructure, consistent with the measured hardness values (~452 to 474 $HV_{0.2}$).

Under differential cooling conditions (Conditions 3–5), Figs. 6(b–d), distinct thermal behaviors are observed between the heated and cooled regions. Increasing tool temperature progressively reduces the local thermal gradient and delays heat extraction in the heated region.

For Condition 3 (100 °C), Fig. 6(b), only a slight deviation in the cooling curve is observed in the heated region, corresponding to a moderate reduction in hardness (~419 $HV_{0.2}$).

For Condition 4 (200 °C), Fig. 6(c), the cooling curve in the heated region enters the bainitic transformation domain for a

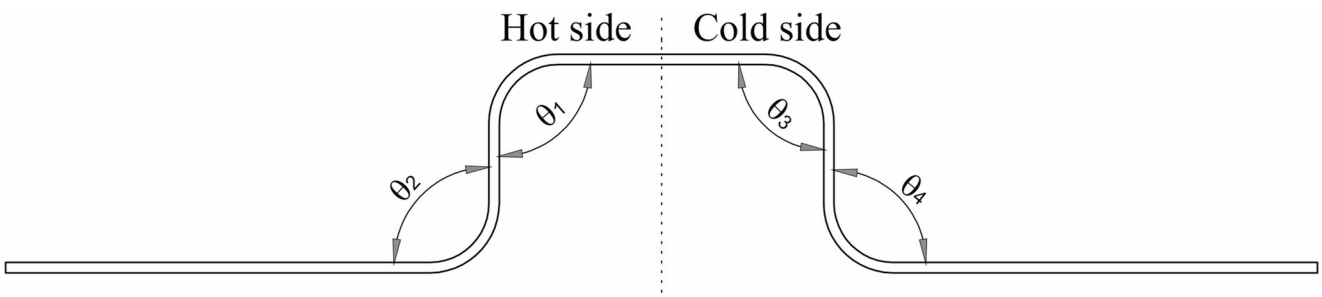

Fig. 5 Definition of the angles measured on the stamped component

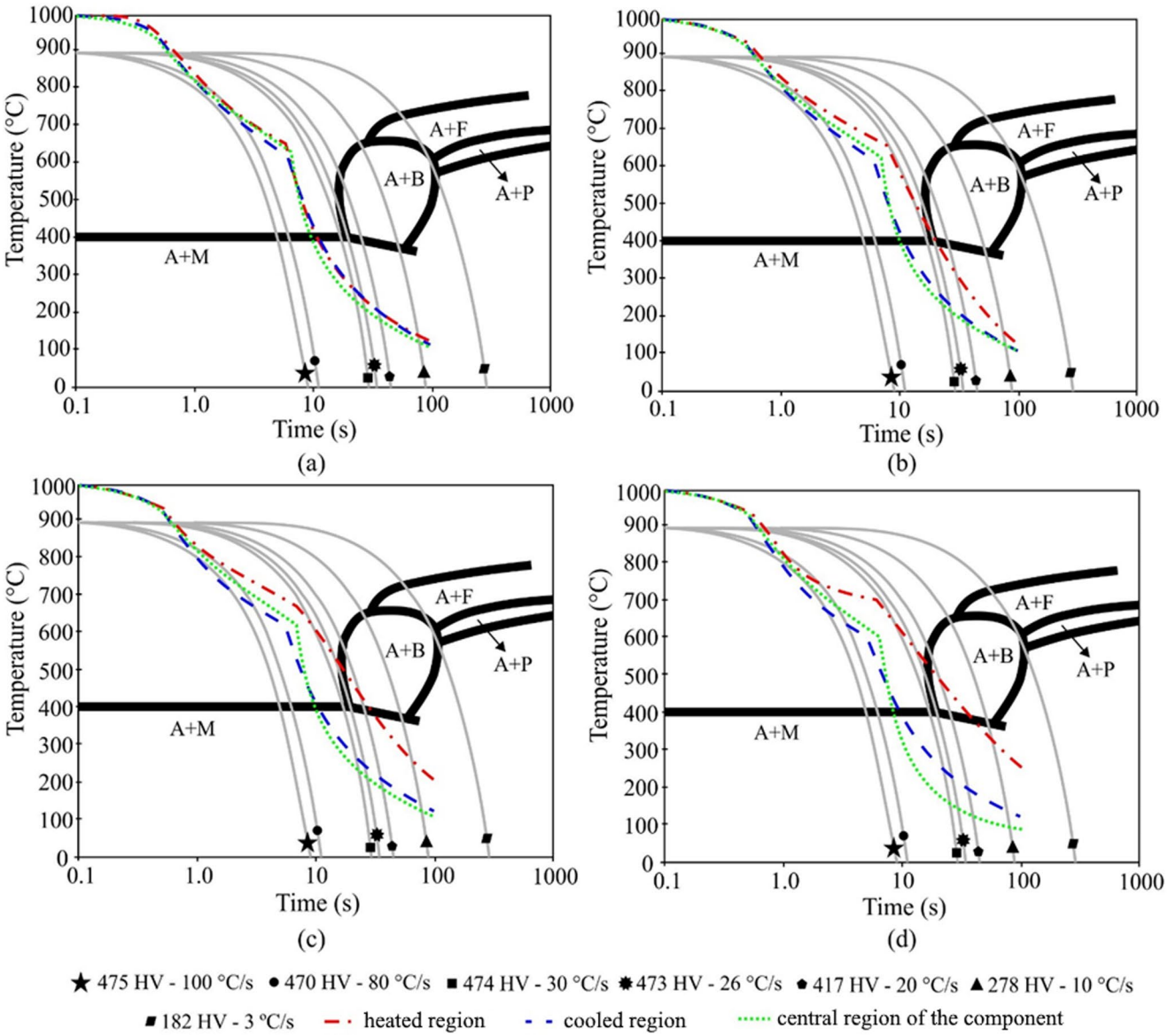

Fig. 6 Transformation diagram for USIBOR® 1500 steel (adopted from literature) superimposed with experimentally measured cooling curves obtained at different locations of the stamped component under hot stamping conditions: (**a**) conventional hot stamping with tools at ambient temperature (Condition 2); (**b**) partial tool heating at 100 °C (Condition 3); (**c**) partial tool heating at 200 °C (Condition 4); and (**d**) partial tool heating at 300 °C (Condition 5). The curves correspond to the heated region, center of the component, and cooled region

longer duration, indicating increased contribution of diffusional transformations and reduced hardness (~373 $HV_{0.2}$).

For Condition 5 (300 °C), Fig. 6(d), the deviation becomes pronounced, with the cooling path remaining in the bainitic region for an extended time, resulting in the lowest hardness (~326 $HV_{0.2}$).

Overall, the results demonstrate that increasing tool temperature leads to a continuous and spatially varying reduction in cooling rate, rather than a discrete thermal boundary [9, 42]. This behavior supports the existence of a transition region governed by progressive changing thermal histories along the component [40].

3.2 Microstructural evolution

The microstructures obtained under the different hot stamping conditions are presented in Figs. 7, 8, 9 and 10. Phase identification is based on the combined analysis of optical features, local hardness values, and the corresponding cooling paths (Fig. 6).

For conventional hot stamping (Condition 2), Fig. 7, all analyzed regions exhibit features consistent with predominantly martensitic microstructures [9, 43], supported by both high cooling rates, Fig. 6(a), and high hardness values.

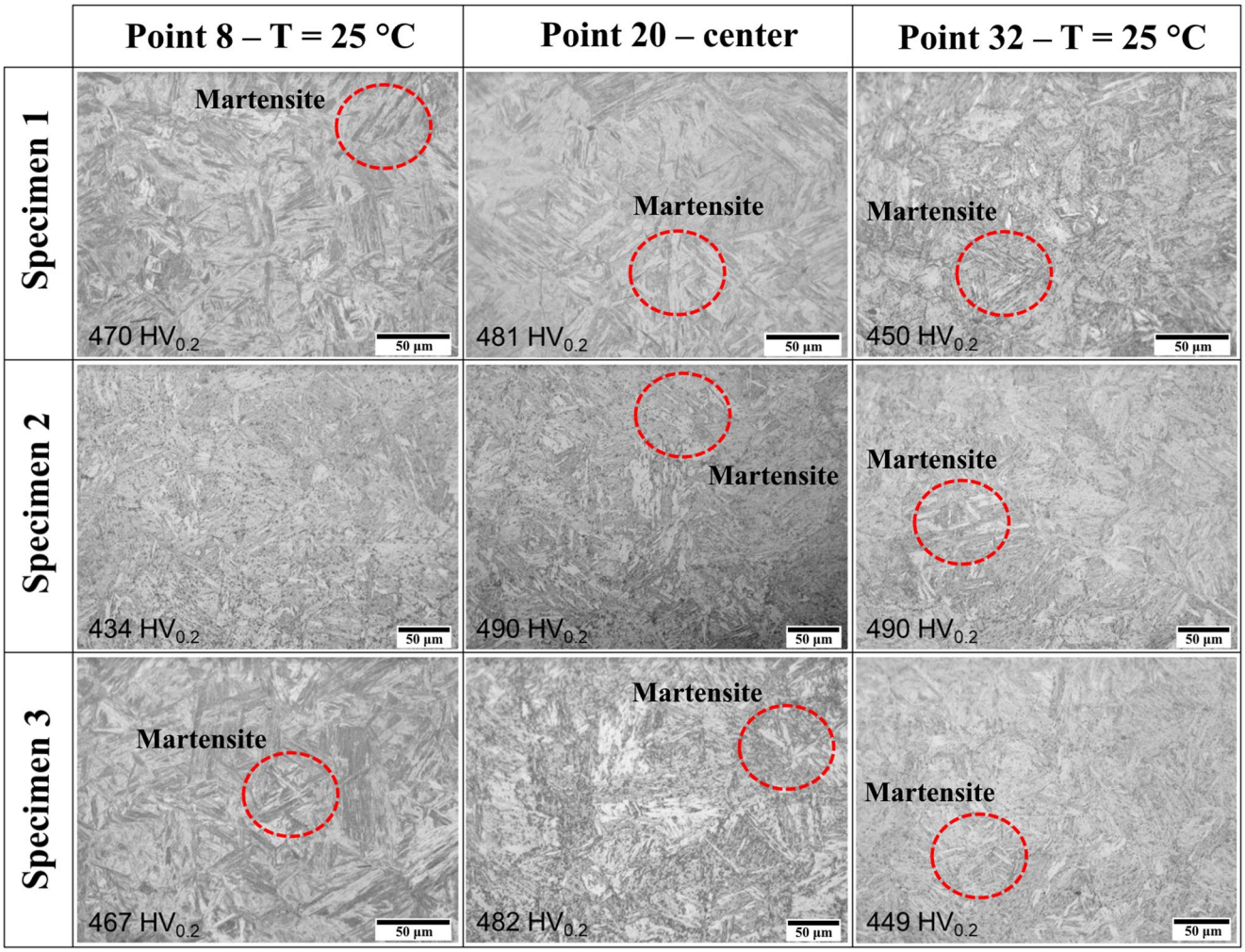

Fig. 7 Optical microstructures of USIBOR® 1500 steel obtained under conventional hot stamping conditions (Condition 2), corresponding to regions adjacent to points 8 (heated side), 20 (center), and 32 (cooled side). All regions exhibit a predominantly martensitic microstructure, consistent with the high cooling rates imposed by unheated tooling. The corresponding microhardness values ($HV_{0.2}$) are indicated

Under partial tool heating at 100 °C (Condition 3), Fig. 8, the heated region shows subtle microstructural modification. Although martensite remains dominant, the reduction in hardness suggests the presence of minor bainitic constituents. The center and cooled regions remain essentially martensitic [40].

For Condition 4 (200 °C), Fig. 9, more pronounced microstructural changes are observed. The heated region exhibits characteristics consistent with mixed martensitic–bainitic microstructures, as indicated by hardness levels and the corresponding cooling paths. The center region shows transitional behavior, while the cooled region remains predominantly martensitic.

For Condition 5 (300 °C), Fig. 10, the heated region exhibits the lowest hardness values and microstructural features consistent with a predominantly bainitic microstructure, possibly containing isolated martensitic constituents. The center and cooled regions exhibit a gradual transition toward higher martensitic fractions [21].

It is important to emphasize that the transition between microstructural states is gradual rather than discrete, reflecting the continuous variation in cooling rates. Furthermore, due to the limitations of optical microscopy under continuous cooling conditions, the phase descriptions should be interpreted as qualitative, based on the combined thermal–mechanical evidence.

3.3 Microhardness distribution

Vickers microhardness profiles were measured along the component for all processing conditions (Fig. 4). For each condition, Fig. 11, three specimens were analyzed, and average values with standard deviations were calculated.

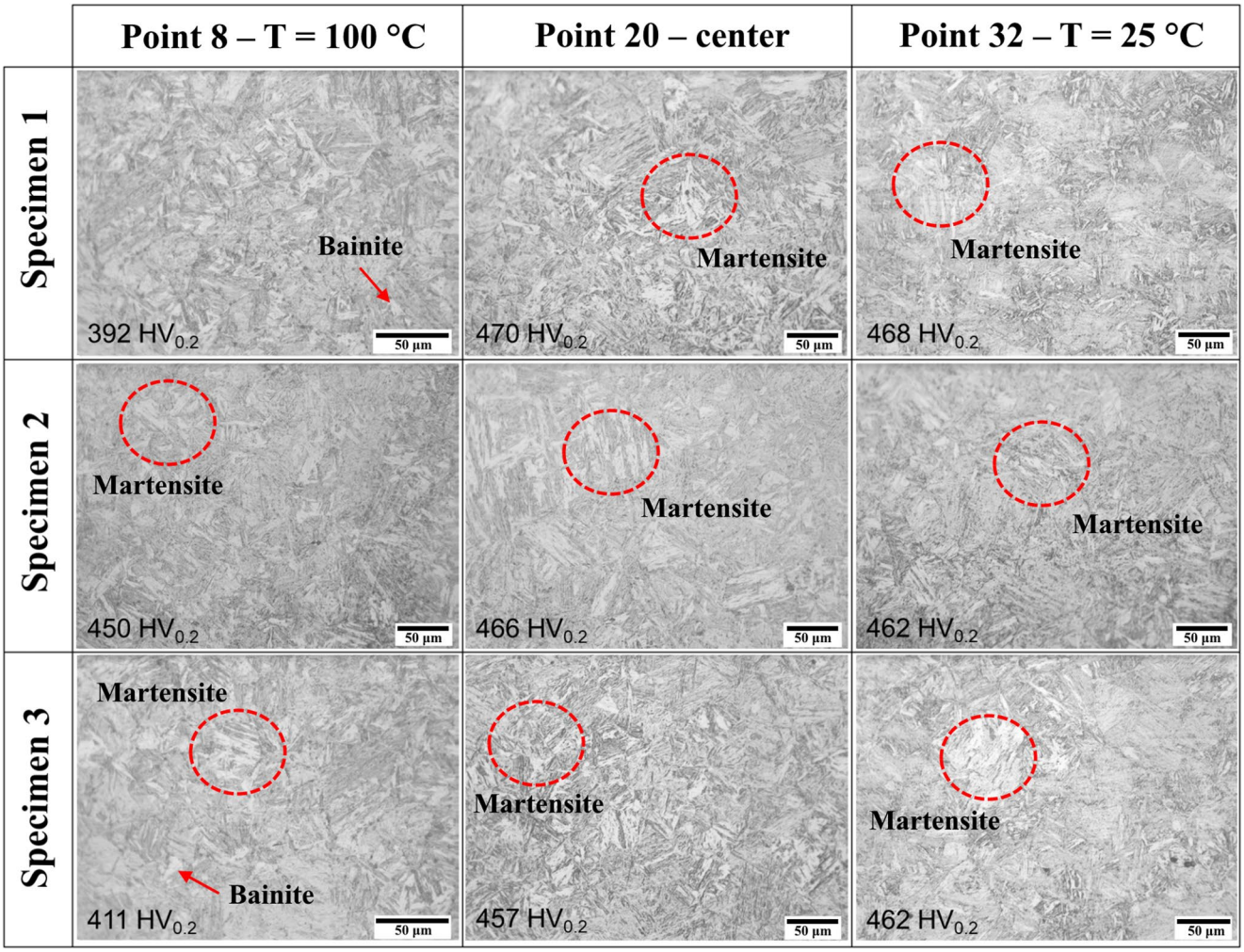

Fig. 8 Optical microstructures of USIBOR® 1500 steel obtained under partial tool heating at 100 °C (Condition 3), corresponding to regions adjacent to points 8 (heated side), 30 (center), and 32 (cooled side). The microstructures are predominantly martensitic, with a slightly reduction microhardness observed in the heated region due to locally reduced cooling rates

A clear correlation between thermal history, phase transformation behavior, and hardness distribution is observed. Regions subjected to higher cooling rates (cooled side) consistently exhibit high hardness values associated with martensitic transformation, whereas regions exposed to reduced cooling rates show progressively lower hardness values.

Under cold stamping conditions (Condition 1), slight hardness variations are observed, with higher values near bending radii. Statistical analysis (Kruskal–Wallis, $p_{\text{-value}} < 0.05$) confirms significant differences between regions.

For conventional hot stamping (Condition 2), the hardness distribution is statistically uniform ($p > 0.05$), with an average value of 474 ± 16 $HV_{0.2}$, reflecting homogeneous thermal conditions and fully martensitic transformation.

Under partial tool heating, a progressive reduction in hardness ($p < 0.05$) is observed in the heated region:

- Condition 3 (100 °C): ~418 ± 22 $HV_{0.2}$). This reduction reflects locally decreased cooling rates and the onset of mixed transformation behavior.
- Condition 4 (200 °C): ~373 ± 25 $HV_{0.2}$). The continuous variation in hardness along the component indicates progressively changing transformation conditions, rather than discrete microstructural boundaries [40].
- Condition 5 (300 °C): ~326 ± 18 $HV_{0.2}$). This behavior is consistent with significantly reduced cooling rates in the heated region [2, 27, 32].

In contrast, the cooled regions maintain high hardness values (~450–470 $HV_{0.2}$) across all conditions.

Importantly, the hardness variation along the component is continuous, without abrupt transitions. This behavior provides strong experimental evidence for the existence of a

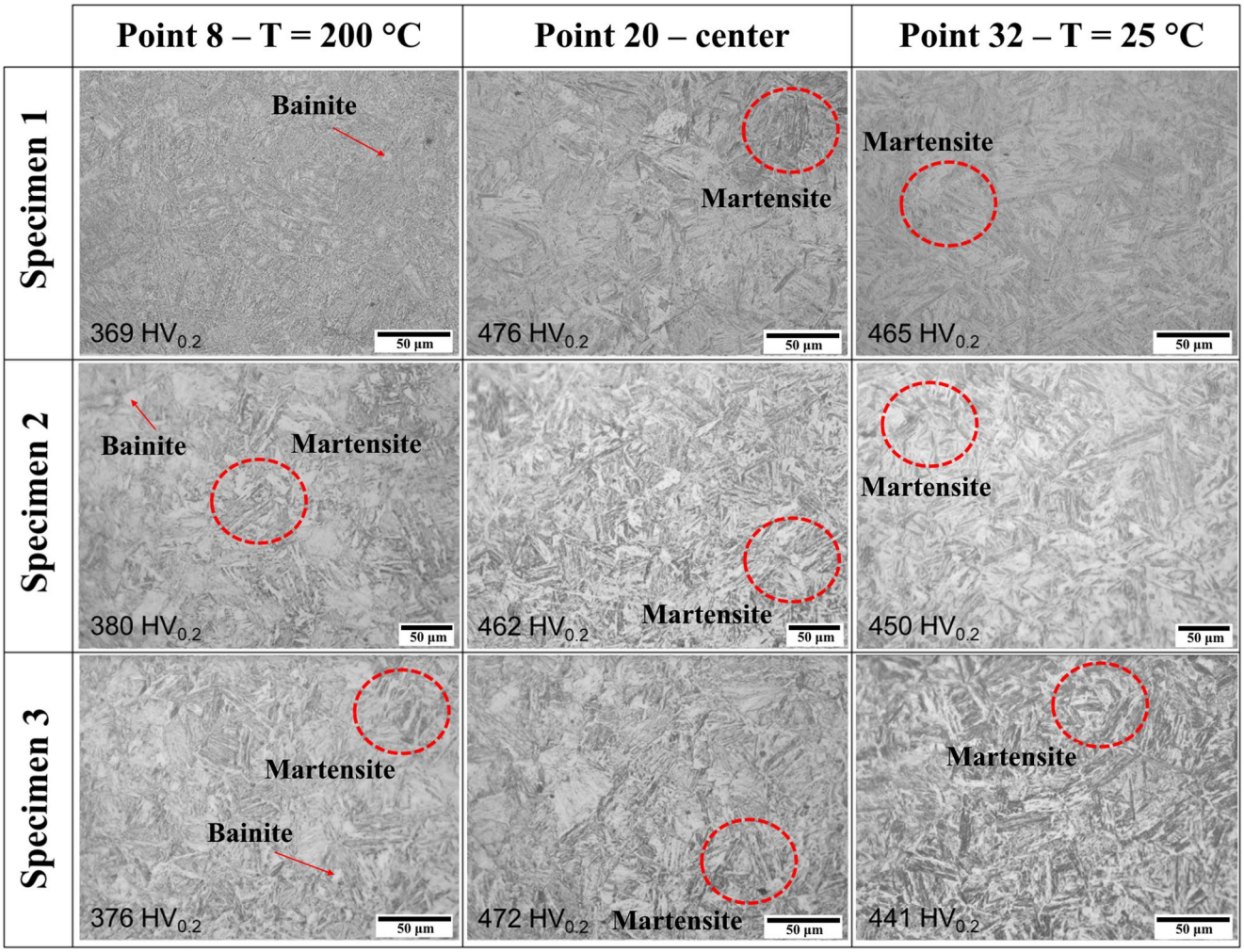

Fig. 9 Optical microstructures of USIBOR® 1500 steel obtained under partial tool heating at 200 °C (Condition 4). The region adjacent to the heated tools (point 9) exhibited a mixed martensitic–bainitic microstructure, whereas the center (point 20) and cooled region (point 32) retain predominantly martensitic microstructures. Corresponding microhardness values ($HV_{0.2}$) are indicated

transition region, governed by gradually changing thermal and transformation conditions.

3.4 Springback behavior

Figure 12 presents the springback values (α_1–α_4) measured at different locations along the component. Compared to cold stamping, all hot stamping conditions significantly reduce springback, resulting in values close to zero. However, under differential heating conditions, a systematic shift toward negative springback is observed in regions associated with the heated tooling.

For angle α_1 (heated side), values remain close to zero for Conditions 1–3, while negative springback becomes evident for Conditions 4 and 5. A similar trend is observed for angle α_2, although with more pronounced variation.

For α_2, a non-monotonic behavior is observed. Under Condition 3 (100 °C), α_2 slightly decreases compared to cold forming. However, for Conditions 4 and 5 (200–300 °C), α_2 increases in magnitude. This behavior results from the competition between two mechanisms:

- At lower tool temperatures (100 °C), thermal softening dominates, promoting more uniform deformation and slightly reducing springback.
- At higher temperatures (200–300 °C), thermal and microstructural gradients become dominant, leading to asymmetric phase transformation and residual stress development.

The increasing asymmetry between heated and cooled regions generates residual stress gradients, promoting

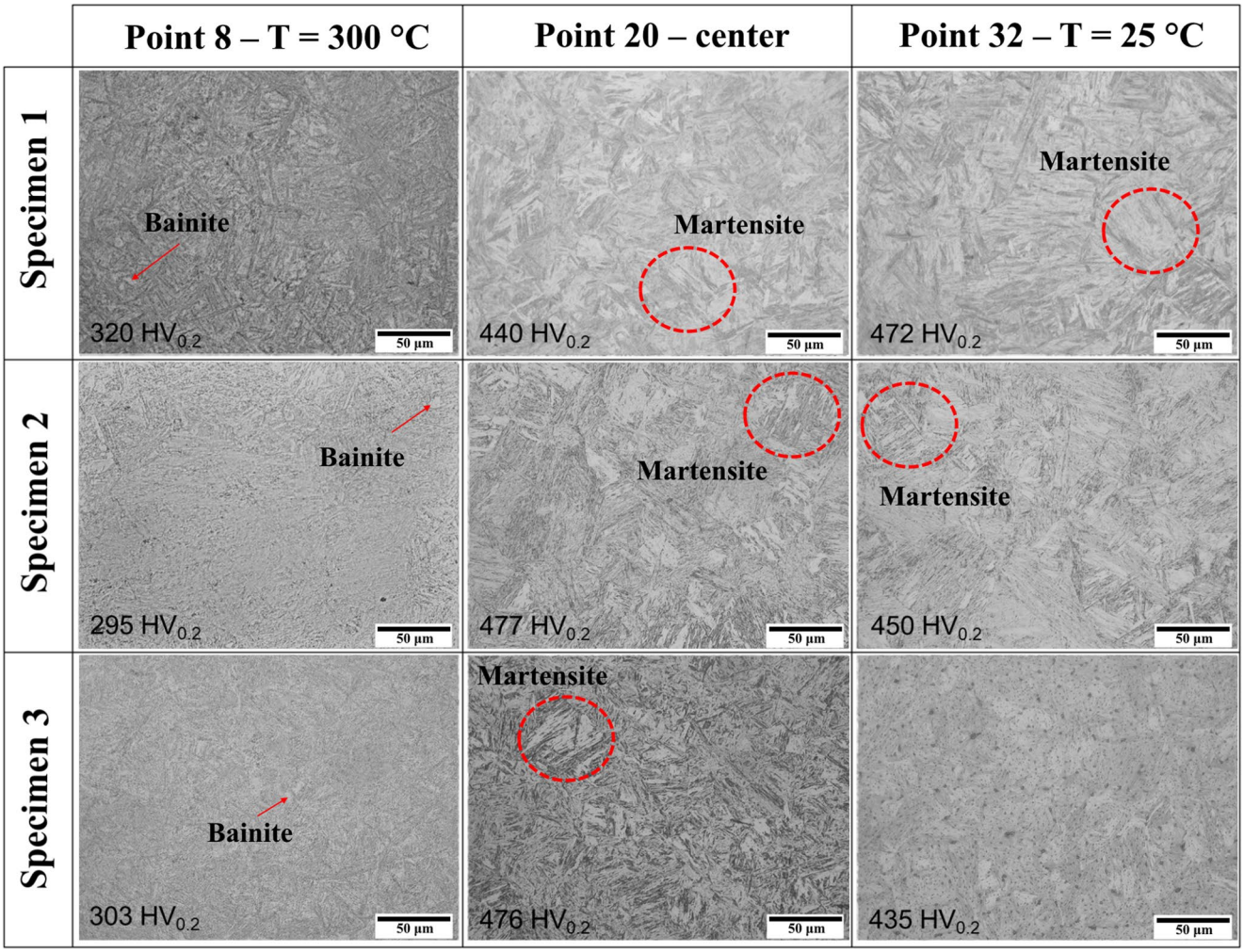

Fig. 10 Optical microstructures of USIBOR® 1500 steel obtained under partial tool heating at 300 °C (Condition 5). The heated region (point 8) exhibits a predominantly bainitic microstructure, possibly containing isolated martensitic islands, while the center (point 20) and cooled region (point 32) remain martensitic. The associated microhardness values ($HV_{0.2}$) are shown

inward angular deviation and, consequently, higher absolute springback values.

In contrast, angles α_3 and α_4 (cooled region) remain close o to zero for all hot stamping conditions, indicating limited sensitivity to thermal gradients.

Although an increase in temperature typically reduces springback under homogeneous conditions (due to reduced elastic modulus and flow stress), this trend does not apply directly to the present case. In differential hot stamping, the response is governed by thermal gradients, phase transformation strains, and residual stress redistribution, rather than by intrinsic temperature-dependent material softening alone [12, 34, 35].

The progressive increase in negative springback with tool temperature is therefore attributed to:

- asymmetric phase transformation (martensite vs. bainite),
- differential thermal contraction,
- and resulting residual stress gradients.

A clear correlation between local hardness and springback is also observed, with lower hardness regions exhibiting higher magnitudes of negative springback.

The observed behavior is consistent with literature data for hot stamping of 22MnB5 steel, where springback typically remains within a narrow range around zero. The results obtained for Condition 2 are in agreement with previously reported values (values between − 0.26° and 0.03° for similar geometries and processing conditions) [44], despite the lower forming temperature (600–650 °C) used in this study.

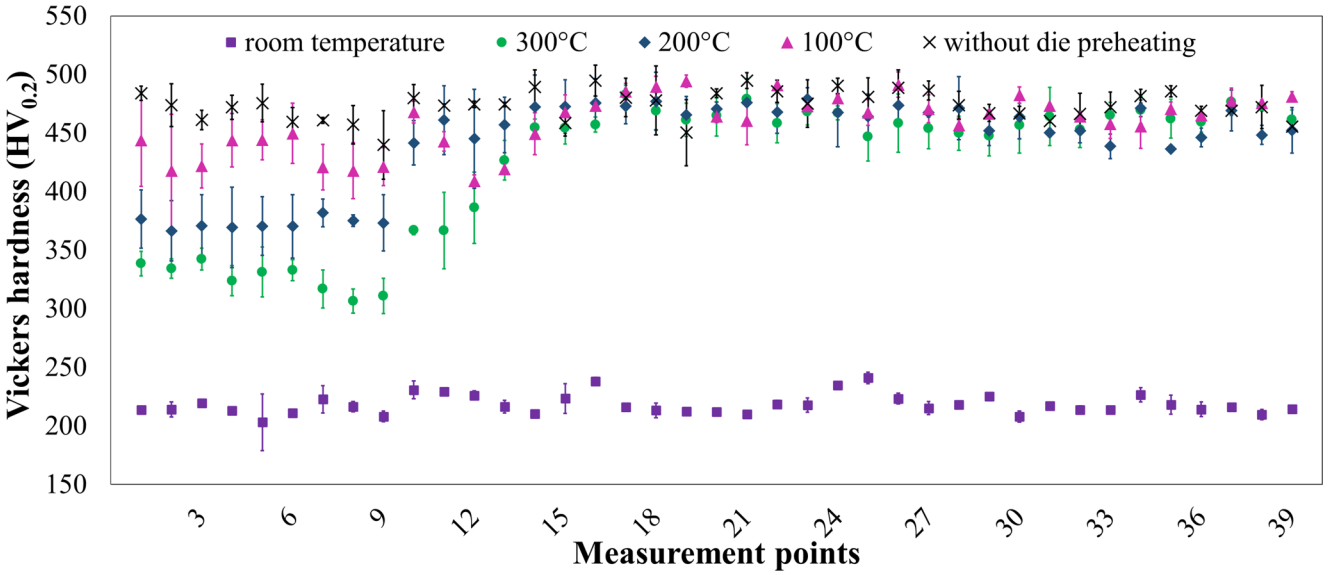

Fig. 11 Vickers microhardness ($HV_{0.2}$) profiles measured along the stamped component for all forming conditions. The results highlight the progressive reduction in microhardness in the heated regions with increasing tool temperature, while the cooled regions maintain high hardness values characteristic of martensitic transformation

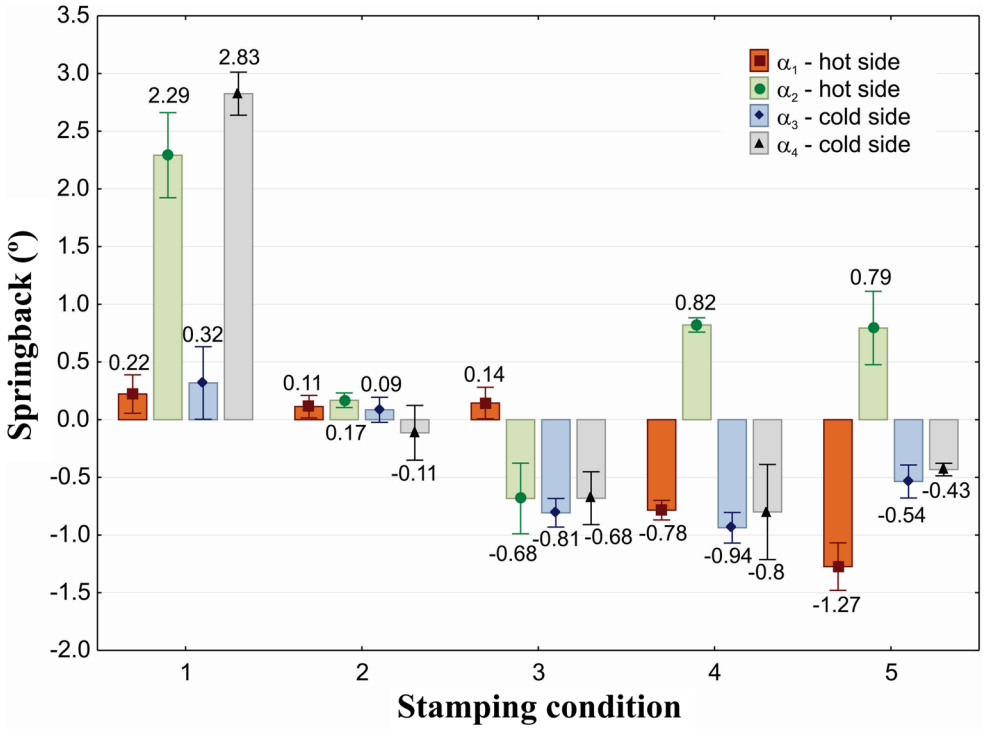

Fig. 12 Springback angles (α_1–α_4) measured at different curvature regions of the stamped component for all forming conditions. Hot stamping significantly reduces springback compared with cold forming, whereas partial tool heating induces a controlled increase in negative springback in the heated regions

The progressive development of negative springback under partial tool heating conditions is attributed to asymmetric thermal and microstructural conditions [34, 35]. The cooled regions, undergoing predominantly martensitic transformation, experience volumetric expansion [10, 27], while the heated regions exhibit reduced transformation strains due to lower cooling rates and mixed microstructures. This mismatch generates residual stresses gradients that promote inward angular deviation after unloading [45].

A clear correlation between local hardness and springback response is also observed, with lower hardness regions exhibiting higher magnitudes of negative springback. Statistical analysis (Table 4) confirms that the stamping condition has a significant effect on all measured angles ($p < 0.05$).

Table 4 Statistical significance (P_{-value}) obtained from analysis of variance (ANOVA)

ANOVA for springback of angle α_1 on the hot side					
Factor	**Sum of squares**	**Degree of freedom**	**Mean square**	**F_{-value}**	**P_{-value}**
Stamping condition	5.4163	4	1.3541	46.7893	0.00*
Error	0.2894	10	0.0289		
Total	5.7057				
ANOVA for springback of angle α_2 on the hot side					
Factor	**Sum of squares**	**Degree of freedom**	**Mean square**	**F_{-value}**	**P_{-value}**
Stamping condition	14.4458	4	3.6115	36.0232	0.00*
Error	1.0025	10	0.1003		
Total	15.4483				
ANOVA for springback of angle α_3 on the cold side					
Factor	**Sum of squares**	**Degree of freedom**	**Mean square**	**F_{-value}**	**P_{-value}**
Stamping condition	5.9804	4	1.4950	25.7626	0.00*
Error	0.5803	10	0.0580		
Total	6.5607				
ANOVA for springback of angle α_4 on the cold side					
Factor	**Sum of squares**	**Degree of freedom**	**Mean square**	**F_{-value}**	**P_{-value}**
Stamping condition	27.1883	4	6.7971	72.7687	0.00*
Error	0.9341	10	0.0934		
Total	28.1224				

*P_{-value} = 0 when results tend to zero

Springback evaluation in this study is based on angular measurements, which provide a robust and widely used metric for comparative analysis in U-bending. However, this approach does not fully capture global geometric deviations. As demonstrated in recent studies [8], small angular variations may coexist with larger full-field distortions. Therefore, while the present methodology reliably captures the main trends, full-field techniques (e.g., 3D scanning) could provide a more comprehensive assessment.

4 Discussion

The experimental results demonstrate that tool temperature is the parameter governing the thermo-mechanical response during differential hot stamping, as it directly controls local cooling rates and, consequently, the phase transformation pathways of USIBOR® 1500 steel [46]. From a process–structure–property perspective, this behavior can be consistently interpreted by considering the role of tool temperature in modifying the interfacial heat transfer conditions at the tool–sheet interface [9, 14], particularly during the initial stages of die quenching, when the majority of heat extraction occurs [24].

As evidenced by the measured cooling curves (Fig. 6), increasing the temperature of the heated tool region reduces the local thermal gradient and delays heat extraction immediately after contact [46]. This leads to a progressive reduction in cooling rate with increasing tool temperature, which directly affects phase transformation kinetics under non-isothermal conditions [9, 14]. The strong correlation between cooling paths, hardness distribution (Fig. 11), and observed microstructural features confirms that the imposed thermal boundary conditions govern the final material response [14].

In addition to the boundary temperature, the effective interfacial heat transfer coefficient (IHTC) is also influenced by the local thermal conditions, contact pressure, and temperature-dependent material properties [46]. Under differential heating conditions, these effects act simultaneously, explaining the high sensitivity of phase transformation behavior to relatively moderate variations in tool temperature (100–300 °C) [2, 29, 32].

From a microstructural standpoint, the results indicate a controlled transition from predominantly martensitic microstructures to mixed martensitic–bainitic and bainitic-dominated conditions in the heated regions [27]. This interpretation is supported by the combined analysis of cooling curves, hardness measurements, and optical observations. However, due to the limitations of optical microscopy under continuous cooling conditions [9, 33, 43], the descriptions “predominantly bainitic” and “mixed martensitic–bainitic” should be interpreted as qualitative.

Importantly, the cooled regions consistently retain high values and microstructural features associated with martensitic transformation, indicating that the imposed thermal gradients remain spatially localized [21, 32]. This behavior confirms the feasibility of tailoring local properties without compromising the structural integrity of the component.

A key outcome of this study is the identification of a transition region between heated and cooled zones [32, 46]. Rather than a sharp interface, both cooling curves and hardness profiles reveal a gradual variation in thermal history and mechanical response over a finite spatial distance [28, 47, 48]. In the present work, this transition region is inferred from continuous hardness gradients and intermediate cooling conditions, rather than directly characterized through high-resolution microstructural techniques.

From a mechanical standpoint, such a transition region is expected to play an important role in stress redistribution during cooling and unloading. The gradual variation in properties may reduce strain incompatibilities between adjacent regions, thereby mitigating localized stress concentrations and contributing to improved dimensional stability [20].

The springback behavior further highlights the strong coupling between thermal history, phase transformation, and mechanical response. While conventional hot stamping leads to near-zero springback due to reduced flow stress and transformation-related stress relaxation [39], the introduction of partial tool heating results in a progressive increase in negative springback in the heated regions.

This behavior can be explained by the asymmetric thermo-metallurgical conditions across the component [20]. The cooled regions, undergoing martensitic transformation, experience volumetric expansion, whereas the heated regions, subjected to lower cooling rates, exhibit reduced transformation strains due to the formation of mixed or bainitic microstructures [14]. This mismatch generates residual stress gradients that promote inward angular deviation after unloading.

In addition, differential thermal contraction during cooling to room temperature further contributes to stress redistribution. As a result, the springback response becomes increasingly governed by these asymmetric effects, rather than by the intrinsic reduction in elastic modulus typically associated with elevated temperatures.

This observation directly addresses an apparent contradiction: although increasing temperature generally reduces springback under homogeneous conditions, the opposite trend is observed here due to the dominance of thermal gradients and phase transformation heterogeneity [34, 35]. Therefore, under differential hot stamping conditions, springback is controlled by spatial variations in thermal and metallurgical states, rather than by temperature-dependent material softening alone [20, 22].

A clear correlation between hardness and springback is also observed, with lower hardness regions exhibiting higher magnitudes of negative springback [9, 39]. This relationship reinforces the process–structure–property framework established in this study.

Although transformation-induced plasticity (TRIP) may occur under such non-isothermal conditions, particularly in regions with mixed transformation products [49, 50], its contribution cannot conclusively assessed, as retained austenite was not directly quantified. Therefore, TRIP is considered a possible secondary mechanism in the present analysis.

Similarly, the influence of prior austenite grain size (PAGS) was not explicitly evaluated. While grain size may affect transformation kinetics, the present results indicate that cooling rate is the dominant factor under the investigated conditions. A more detailed assessment would require advanced characterization techniques such as EBSD and is recommended for future work.

From a modeling perspective, the observed behavior can also be interpreted in light of recent advances in constitutive modeling of sheet metals. In cold forming, accurate springback prediction requires detailed representation of anisotropy, kinematic hardening, and distortional hardening effects, as demonstrated in recent studies [6–8]. These models capture the evolution of the yield surface during deformation and unloading, which is critical for predicting elastic recovery.

In contrast, under hot stamping conditions, the dominant mechanisms governing springback shift toward thermally driven effects, including temperature-dependent flow behavior, phase transformation strains, and residual stress evolution [9, 36, 45]. As a result, the relative importance of advanced constitutive modeling is reduced, while thermo-metallurgical coupling becomes the controlling factor.

The present results are consistent with this framework, as the observed reduction, inversion, and spatial variation of springback are associated with asymmetric cooling conditions and transformation-induced strain gradients, rather than purely mechanical hardening effects [18, 27].

Finally, it should be noted that springback evaluation in this study is based on angular measurements, which provide a reliable and widely adopted metric for comparative analysis in U-bending configurations. However, this approach does not fully capture global geometric deviations. As highlighted in recent studies, small angular variations may not reflect the full deformation field, which may require full-field techniques such as 3D scanning [6, 8].

Therefore, while the adopted methodology enables consistent comparison between processing conditions and clearly captures the influence of thermal gradients, future studies could benefit from full-field characterization methods to provide a more comprehensive assessment of springback behavior.

Overall, the combined use of real-time thermal measurements, hardness mapping, and microstructural observations provides a consistent and experimentally supported framework for interpreting differential hot stamping under non-isothermal conditions. The results demonstrate that partial tool heating enables controlled tailoring of microstructure, mechanical properties, and springback behavior within a single forming operation.

5 Conclusions

Based on the experimental investigation of USIBOR® 1500 steel subjected to differential hot stamping with partial tool heating, the following conclusions can be drawn:

(1) Tool temperature is the primary parameter controlling local cooling rates during differential hot stamping. Increasing the tool temperature from 100 to 300 °C

progressively reduces the cooling rates in the heated regions, while maintaining rapid quenching in the cooled regions.

(2) A consistent relationship between thermal history, phase transformation behavior, and hardness distribution was established. Reduced cooling rates promoted the formation of mixed transformation products, leading to a systematic decrease in hardness, whereas the cooled regions retained high hardness associated with predominantly martensitic transformation.

(3) Partial tool heating enables the development of a controlled microstructural gradient across the component, evolving from predominantly martensitic to mixed martensitic–bainitic and bainitic-dominated regions. These descriptions are based on combined thermal, hardness, and optical microscopy analysis and should be interpreted as qualitative.

(4) The imposed thermal gradients resulted in smooth and continuous hardness variations along the component, with differences exceeding 120 $HV_{0.2}$. This behavior supports the presence of a transition region governed by progressively varying thermal conditions, inferred from thermal and mechanical evidence.

(5) Hot stamping significantly reduces springback compared with cold forming. Partial tool heating promotes a mensurable shift toward negative springback in the heated regions, while the cooled regions remain close to zero springback.

(6) The observed springback behavior is governed by the combined effects of differential thermal contraction and phase transformation-induced strains under non-isothermal conditions. The contribution of transformation-induced plasticity (TRIP) cannot be confirmed and is considered secondary.

Overall, the results demonstrated that differential cooling using partial tool heating provides an effective and controllable strategy for tailoring local microstructure, hardness, and springback behavior within a single forming operation. The study establishes an experimentally supported process–structure–property relationships, contributing to the development of advanced press-hardened steel components with spatially tailored performance.

Acknowledgements C.P. Lisboa acknowledges the *Conselho Nacional de Desenvolvimento Científico e Tecnológico (CNPq)* for the financial support provided through a master's scholarship. R.L. Dalcin acknowledges the financial support provided by the *Fundação de Amparo à Pesquisa do Estado do Rio Grande do Sul (FAPERGS)* [Process no. 24/2551-0000770-9] and [Process no. 25/2551-0002892-2].

Author contributions All authors contributed to the conception and design of the study C.P. Lisboa at the time of the experimental development of this work, was a Master's student at PPGE3M of the Federal University of Rio Grande do Sul (UFRGS), under the guidance of L. Schaeffer, then Full Professor at UFRGS and supervisor of PPGE3M. A. Rosiak performed the metallographic analyses. J.B. Ercolani and R.S. Ramalho assisted with the experimental setup, specimen handling, and monitoring during the forming tests. R.T. Lermen carried out the statistical analysis and contributed to the drafting and critical revision of the manuscript. R.L. Dalcin wrote the initial version of the manuscript. All authors reviewed and approved the final manuscript.

Funding The Article Processing Charge (APC) for the publication of this research was funded by the Coordenação de Aperfeiçoamento de Pessoal de Nível Superior - Brasil (CAPES) (ROR identifier: 00x0ma614).

Data availability The datasets generated and/or analyzed during the current study are available from the corresponding author on reasonable request.

Declarations

Conflict of interest The authors declare no conflict of interest.

References

1. Demeri MY (2013) Advanced-High Strength Steels: Science, Technology, and Applications. ASM International
2. Park J-M, Son S-G, Park K-J et al (2025) Investigation of tailored softening behavior of aluminized boron steel (22MnB5) in hot stamping process using die surface relief patterns. J Manuf Process 150:1097–1107. https://doi.org/10.1016/j.jmapro.2025.06.067
3. Zhao J, Jiang Z (2018) Thermomechanical processing of advanced high strength steels. Prog Mater Sci 94:174–242. https://doi.org/10.1016/j.pmatsci.2018.01.006
4. Pereira R, Peixinho N, Costa SL (2024) A Review of Sheet Metal Forming Evaluation of Advanced High-Strength Steels (AHSS). Metals 14:394. https://doi.org/10.3390/met14040394
5. Ilyas Kacar F, Ozturk F Jarrar (2021) Defects and Remedies in Stamping of Advanced High Strength Steels. J Mod Mech Eng Technol 1:68–74. https://doi.org/10.15377/2409-9848.2014.01.02.4
6. Choi J, Lee J, Bong HJ et al (2018) Advanced constitutive modeling of advanced high strength steel sheets for springback prediction after double stage U-draw bending. Int J Solids Struct 151:152–164. https://doi.org/10.1016/j.ijsolstr.2017.09.030
7. Hu Q, Maier L, Nishiwaki T et al (2024) User friendly FE Formulation for anisotropic distortional hardening model based on non-associated flow plasticity and its application to springback prediction. Thin-Walled Struct 202:112142. https://doi.org/10.1016/j.tws.2024.112142

8. Firat M, Esener E, Akşen TA (2025) The role of polynomial yield criteria in accurate simulation of bending deformation in thin-walled steel structures. EC 42:1791–1824. https://doi.org/10.1108/EC-12-2024-1072
9. Hart-Rawung T, Buhl J, Horn A et al (2023) A unified model for isothermal and non-isothermal phase transformation in hot stamping of 22MnB5 steel. J Mater Process Technol 313:117856. https://doi.org/10.1016/j.jmatprotec.2023.117856
10. Karbasian H, Tekkaya AE (2010) A review on hot stamping. J Mater Process Technol 210:2103–2118. https://doi.org/10.1016/j.jmatprotec.2010.07.019
11. Zhu B, Zhu Z, Jin Y et al (2019) Multilayered-Sheet Hot Stamping and Application in Electric-Power-Fitting Products. Metals 9:215. https://doi.org/10.3390/met9020215
12. Wang A, Zhong K, El Fakir O et al (2017) Springback analysis of AA5754 after hot stamping: experiments and FE modelling. Int J Adv Manuf Technol 89:1339–1352. https://doi.org/10.1007/s00170-016-9166-3
13. Bariani PF, Bruschi S, Ghiotti A, Turetta A (2008) Testing formability in the hot stamping of HSS. CIRP Ann 57:265–268. https://doi.org/10.1016/j.cirp.2008.03.049
14. Sun H, Yao S, Tang Q et al (2024) Short-wave infrared heating of 22MnB5 steel with adjusted surface emissivity for press hardening of tailored-strength components. J Manuf Process 120:74–85. https://doi.org/10.1016/j.jmapro.2024.04.032
15. Abdollahpoor A, Chen X, Pereira MP et al (2016) Sensitivity of the final properties of tailored hot stamping components to the process and material parameters. J Mater Process Technol 228:125–136. https://doi.org/10.1016/j.jmatprotec.2014.11.033
16. Merklein M, Wieland M, Lechner M et al (2016) Hot stamping of boron steel sheets with tailored properties: A review. J Mater Process Technol 228:11–24. https://doi.org/10.1016/j.jmatprotec.2015.09.023
17. Mori K, Suzuki Y, Yokoo D et al (2020) Steel sheets partnered with quenchable sheet in hot stamping of tailor-welded blanks and its application to separation prevention of fractured components. Int J Adv Manuf Technol 111:725–734. https://doi.org/10.1007/s00170-020-06100-4
18. George R, Bardelcik A, Worswick MJ (2012) Hot forming of boron steels using heated and cooled tooling for tailored properties. J Mater Process Technol 212:2386–2399. https://doi.org/10.1016/j.jmatprotec.2012.06.028
19. Omer K, George R, Bardelcik A et al (2018) Development of a hot stamped channel section with axially tailored properties – experiments and models. Int J Mater Form 11:149–164. https://doi.org/10.1007/s12289-017-1338-7
20. Votava F, Jirková H, Kučerová L, Jeníček Š (2023) Study of Transition Areas in Press-Hardened Steels in a Combined Tool for Hot and Cold Forming. Materials 16:442. https://doi.org/10.3390/ma16010442
21. Li X, Xiao L, Zheng Q et al (2019) Study on Microstructure and Properties of Tailored Hot-Stamped U-shaped Parts Based on Temperature Field Control. Metals 9:593. https://doi.org/10.3390/met9050593
22. Zhou J, Yang X, Mu Y et al (2021) Numerical simulation and experimental investigation of tailored hot stamping of boron steel by partial heating. J Mater Res Technol 14:1347–1365. https://doi.org/10.1016/j.jmrt.2021.07.025
23. Li H, Wu X, Li G (2013) Prediction of Forming Limit Diagrams for 22MnB5 in Hot Stamping Process. J Materi Eng Perform 22:2131–2140. https://doi.org/10.1007/s11665-013-0491-5
24. Ikeuchi K, Yanagimoto J (2011) Valuation method for effects of hot stamping process parameters on product properties using hot forming simulator. J Mater Process Technol 211:1441–1447. https://doi.org/10.1016/j.jmatprotec.2011.03.017
25. Zhang Z, Yu J, Meng S et al (2018) Effect of Tool Temperature on Microstructure and Properties of Tailored Hot Stamping Components. J Materi Eng Perform 27:4838–4845. https://doi.org/10.1007/s11665-018-3581-6
26. Li N, Lin J, Balint DS, Dean TA (2016) Modelling of austenite formation during heating in boron steel hot stamping processes. J Mater Process Technol 237:394–401. https://doi.org/10.1016/j.jmatprotec.2016.06.006
27. Xu Y, Ji Q, Yang G et al (2020) Effect of Cooling Path on Microstructures and Hardness of Hot-Stamped Steel. Metals 10:1692. https://doi.org/10.3390/met10121692
28. Venturato G, Novella M, Bruschi S et al (2017) Effects of Phase Transformation in Hot Stamping of 22MnB5 High Strength Steel. Procedia Eng 183:316–321. https://doi.org/10.1016/j.proeng.2017.04.045
29. Reitz A, Grydin O, Schaper M (2022) Influence of thermomechanical processing on the microstructural and mechanical properties of steel 22MnB5. Mater Sci Engineering: A 838:142780. https://doi.org/10.1016/j.msea.2022.142780
30. Kulakov M, Poole WJ, Militzer M (2014) A Microstructure Evolution Model for Intercritical Annealing of a Low-carbon Dual-phase Steel. ISIJ Int 54:2627–2636. https://doi.org/10.2355/isijinternational.54.2627
31. Palmieri ME, Villa M, Tricarico L (2025) Microstructure and Properties of Low- and Medium-C Press-Hardened Steels During Hot Stamping with Intermediate Pre-cooling Stage Tailored Process. Metall Mater Trans A 56:1749–1760. https://doi.org/10.1007/s11661-025-07742-3
32. Golovko O, Stolte M-H, Wölki K et al (2020) Tailoring Soft Local Zones in Quenched Blanks of the Steel 22MnB5 by Partial Pre-cooling with Compressed Air. J Materi Eng Perform 29:4379–4389. https://doi.org/10.1007/s11665-020-04916-5
33. Golling S, Frómeta D, Casellas D, Jonsén P (2019) Influence of microstructure on the fracture toughness of hot stamped boron steel. Mater Sci Engineering: A 743:529–539. https://doi.org/10.1016/j.msea.2018.11.080
34. Yanagimoto J, Oyamada K, Nakagawa T (2005) Springback of High-Strength Steel after Hot and Warm Sheet Formings. CIRP Ann 54:213–216. https://doi.org/10.1016/S0007-8506(07)60086-9
35. Nakagawa Y, Mori K, Maeno T (2018) Springback-free mechanism in hot stamping of ultra-high-strength steel parts and deformation behaviour and quenchability for thin sheet. Int J Adv Manuf Technol 95:459–467. https://doi.org/10.1007/s00170-017-1203-3
36. Morel X, Mercier S, Bouscaud D et al (2025) Residual stresses in the new press-hardening steels: Experiments and numerical simulations of V-bendings. Mater Today Commun 44:111903. https://doi.org/10.1016/j.mtcomm.2025.111903
37. Merklein M, Lechler J (2006) Investigation of the thermo-mechanical properties of hot stamping steels. J Mater Process Technol 177:452–455. https://doi.org/10.1016/j.jmatprotec.2006.03.233
38. ASTM E8/E8M (2016) Test Methods for Tension. Testing of Metallic Materials
39. Li X, Yan X, Zhang Z (2019) Springback Prediction of a Hot Stamping Component Based on the Area Fractions of Phases. Metals 9:694. https://doi.org/10.3390/met9060694
40. Wojtacha A, Kozłowska A, Morawiec M, Opiela M (2025) Thermodynamic prediction and experimental verification of phase transformation kinetics in 3Mn steel with Ti and V microadditions. J Therm Anal Calorim 150:1081–1091. https://doi.org/10.1007/s10973-024-13578-7
41. Jia T, Militzer M (2015) The Effect of Solute Nb on the Austenite-to-Ferrite Transformation. Metall Mater Trans A 46A:614–621. https://doi.org/10.1007/s11661-014-2659-5
42. Wróbel I, Skowronek A, Grajcar A (2022) A Review on Hot Stamping of Advanced High-Strength Steels:

Technological-Metallurgical Aspects and Numerical Simulation. Symmetry 14:969. https://doi.org/10.3390/sym14050969
43. Naderi M, Saeed-Akbari A, Bleck W (2008) The effects of non-isothermal deformation on martensitic transformation in 22MnB5 steel. Mater Sci Engineering: A 487:445–455. https://doi.org/10.1016/j.msea.2007.10.057
44. Liu H, Liu W, Bao J et al (2011) Numerical and Experimental Investigation into Hot Forming of Ultra High Strength Steel Sheet. J Materi Eng Perform 20:1–10. https://doi.org/10.1007/s11665-010-9641-1
45. Uebing S, Brands D, Scheunemann L, Schröder J (2021) Residual stresses in hot bulk formed parts: two-scale approach for austenite-to-martensite phase transformation. Arch Appl Mech 91:545–562. https://doi.org/10.1007/s00419-020-01836-7
46. Caron EJFR, Daun KJ, Wells MA (2014) Experimental heat transfer coefficient measurements during hot forming die quenching of boron steel at high temperatures. Int J Heat Mass Transf 71:396–404. https://doi.org/10.1016/j.ijheatmasstransfer.2013.12.039
47. Li Y, Chen Y, Li S (2021) Phase transformation testing and modeling for hot stamping of boron steel considering the effect of the prior austenite deformation. Mater Sci Engineering: A 821:141447. https://doi.org/10.1016/j.msea.2021.141447
48. Quan G-Z, Yu Y-Z, Zhang Y et al (2022) A Tailored Preparation Method of Variable Strength for Ultra-High-Strength Steel Sheet and Mapping Mechanism between Process and Property. Materials 15:6620. https://doi.org/10.3390/ma15196620
49. Pornputsiri N, Kanlayasiri K (2020) Effect of bending temperatures on the microstructure and springback of a TRIP steel sheet. Def Technol 16:980–987. https://doi.org/10.1016/j.dt.2019.11.018
50. Behrens B-A, Bouguecha A, Bonk C, Chugreev A (2017) Experimental investigations on the transformation-induced plasticity in a high tensile steel under varying thermo-mechanical loading. cmms 17:36–43. https://doi.org/10.7494/cmms.2017.1.0573